NACA

RESEARCH MEMORANDUM

LIFT, DRAG, AND PITCHING MOMENT OF LOW-ASPECT-RATIO WINGS AT SUBSONIC AND SUPERSONIC SPEEDS - PLANE 45° SWEPT-BACK WING OF ASPECT RATIO 3, TAPER RATIO 0.4 WITH 3-PERCENT-THICK, BICONVEX SECTION

By John C. Heitmeyer

Ames Aeronautical Laboratory
Moffett Field, Calif.

NATIONAL ADVISORY COMMITTEE
FOR AERONAUTICS

WASHINGTON
September 20, 1951

NATIONAL ADVISORY COMMITTEE FOR AERONAUTICS

RESEARCH MEMORANDUM

LIFT, DRAG, AND PITCHING MOMENT OF LOW-ASPECT-RATIO WINGS AT SUBSONIC AND SUPERSONIC SPEEDS - PLANE 45° SWEPT-BACK WING OF ASPECT RATIO 3, TAPER RATIO 0.4 WITH 3-PERCENT-THICK, BICONVEX SECTION

By John C. Heitmeyer

SUMMARY

A wing-body combination having a plane 45° swept-back wing of aspect ratio 3, taper ratio 0.4, and 3-percent-thick biconvex sections in streamwise planes has been investigated at both subsonic and supersonic Mach numbers. The lift, drag, and pitching moment of the model are presented for Mach numbers from 0.60 to 0.92 and from 1.20 to 1.70 at a Reynolds number of 3.83 million. The variations of the characteristics with Reynolds number are also shown for several Mach numbers.

INTRODUCTION

A research program is in progress at the Ames Aeronautical Laboratory to ascertain experimentally at subsonic and supersonic Mach numbers the characteristics of wings of interest in the design of high-speed fighter airplanes. The effects of variations in plan form, twist, camber, and thickness are being investigated. This report is one of a series pertaining to this program and presents results of tests of a wing-body combination having a plane 45° swept-back wing of aspect ratio 3, taper ratio of 0.4, and 3-percent-thick biconvex sections in streamwise planes. Results of other investigations in this program are presented in references 1 to 11. As in these references, the data herein are presented without analysis to expedite publication.

NOTATION

b	wing span
$\bar{c}$	mean aerodynamic chord $\left(\frac{\int_0^{b/2} c^2 dy}{\int_0^{b/2} c \, dy} \right)$
c	local wing chord
l	length of body including portion removed to accommodate sting, inches
$\frac{L}{D}$	lift-drag ratio
$\left(\frac{L}{D}\right)_{max}$	maximum lift-drag ratio
M	Mach number
q	free-stream dynamic pressure
R	Reynolds number based on the mean aerodynamic chord
r	radius of body
r_o	maximum body radius
S	total wing area, including area formed by extending leading and trailing edges to plane of symmetry
x	longitudinal distance from nose of body
y	distance perpendicular to plane of symmetry
α	angle of attack of body axis, degrees
C_D	drag coefficient $\left(\frac{\text{drag}}{qS} \right)$
C_L	lift coefficient $\left(\frac{\text{lift}}{qS} \right)$

C_m pitching-moment coefficient referred to quarter point of mean aerodynamic chord $\left(\frac{\text{pitching moment}}{qS\bar{c}}\right)$

$\frac{dC_L}{d\alpha}$ slope of the lift curve measured at zero lift, per degree

$\frac{dC_m}{dC_L}$ slope of the pitching-moment curve measured at zero lift

APPARATUS

Wind Tunnel and Equipment

The experimental investigation was conducted in the Ames 6- by 6-foot supersonic wind tunnel. In this wind tunnel, the Mach number can be varied continuously and the stagnation pressure can be regulated to maintain a given test Reynolds number. The air is dried to prevent formation of condensation shocks. Further information on this wind tunnel is presented in reference 12.

The model was sting mounted in the tunnel, the diameter of the sting being about 93 percent of the diameter of the body base. The pitch plane of the model support was horizontal. A 4-inch-diameter, four-component, strain-gage balance, enclosed within the body of the model, was used to measure the aerodynamic forces and moments. This balance is described in greater detail in reference 13.

Model

A plan and a front view of the model and certain model dimensions are given in figure 1. The important geometric characteristics of the model are as follows:

Wing

Aspect ratio	3
Taper ratio	0.4
Airfoil section (streamwise)	3-percent-thick, biconvex
Total area, S, square feet	2.425
Mean aerodynamic chord, $\bar{c}$, feet	0.956
Dihedral, degrees	0
Camber	None
Twist, degrees	0
Incidence, degrees	0
Distance, wing-chord plane to body axis, feet	0

Body

Fineness ratio (based upon length l; fig. 1)	12.5
Cross-section shape	Circular
Maximum cross-sectional area, square feet	0.1235
Ratio of maximum cross-sectional area to wing area	0.0509

The wing was constructed of solid steel. The body spar was also steel and was covered with aluminum to form the body contours. The surfaces of the wing and body were polished smooth.

TESTS AND PROCEDURE

Range of Test Variables

The characteristics of the model (as a function of angle of attack) were investigated for a range of Mach numbers from 0.60 to 0.92 and from 1.20 to 1.70. The major portion of the data was obtained at a Reynolds number of 3.83 million. Data were also obtained for Reynolds numbers of 1.53 million and 2.46 million at Mach numbers of 0.60, 0.90, 1.20, and 1.70.

Reduction of Data

The test data have been reduced to standard NACA coefficient form. Factors which could affect the accuracy of these results, together with the corrections applied, are discussed in the following paragraphs.

Tunnel-wall interference.- Corrections to the subsonic results for the induced effects of the tunnel walls resulting from lift on the model were made according to the methods of reference 14. The numerical

values of these corrections (which were added to the uncorrected data) were:

$$\Delta\alpha = 0.554\ C_L$$

$$\Delta C_D = .00967\ C_L^2$$

No corrections were made to the pitching-moment coefficients.

The effects of constriction of the flow at subsonic speeds by the tunnel walls were taken into account by the method of reference 15. This correction was calculated for conditions at zero angle of attack and was applied throughout the angle-of-attack range. At a Mach number of 0.90, this correction amounted to a 2-percent increase in the Mach number and in the dynamic pressure over that determined from a calibration of the wind tunnel without a model in place.

For the tests at supersonic speeds, the reflection from the tunnel walls of the Mach wave originating at the nose of the body did not cross the model. No corrections were required, therefore, for tunnel-wall effects.

Stream variation.- Tests at subsonic speeds in the 6- by 6-foot supersonic wind tunnel of the present symmetrical model in both the normal and the inverted positions have indicated a stream inclination of -0.05° and a stream curvature capable of producing a pitching-moment coefficient of -0.004 at zero lift. No corrections were made to the data of the present report for the effect of these stream irregularities. No measurements have been made of the stream curvature in the yaw plane. At subsonic speeds, the longitudinal variation of static pressure in the region of the model is not known accurately at present, but a preliminary survey has indicated that it is less than 2 percent of the dynamic pressure. No correction for this effect was made.

A survey of the air stream in the 6- by 6-foot wind tunnel at supersonic speeds (reference 12) has shown a stream curvature only in the yaw plane of the model. The effects of this curvature on the measured characteristics of the present model are not known, but are believed to be small as judged by the results of reference 16. The survey (reference 12) also indicated that there is a static-pressure variation in the test section of sufficient magnitude to affect the drag results. A correction was added to the measured drag coefficient, therefore, to account for the longitudinal buoyance caused by this static-pressure variation. This correction varied from as much as -0.0008 at a Mach number of 1.30 to 0.0006 at a Mach number of 1.70.

Support interference.- At subsonic speeds, the effects of support interference on the aerodynamic characteristics of the model are not

known. For the present tailless model, it is believed that such effects consisted primarily of a change in the pressure at the base of the model. In an effort to correct at least partially for this support interference, the base pressure was measured and the drag data were adjusted to correspond to a base pressure equal to the static pressure of the free stream.

At supersonic speeds, the effects of support interference of a body-sting configuration similar to that of the present model are shown by reference 17 to be confined to a change in base pressure. The previously mentioned adjustment of the drag for base pressure, therefore, was applied at supersonic speeds.

RESULTS

The results are presented in this report without analysis in order to expedite publication. The variation of lift coefficient with angle of attack and the variation of drag coefficient, pitching-moment coefficient, and lift-drag ratio with lift coefficient at a Reynolds number of 3.83 million and at Mach numbers from 0.60 to 1.70 are shown in figure 2. The effects of Reynolds number on the aerodynamic characteristics at Mach numbers of 0.60, 0.90, 1.20, and 1.70 are shown in figure 3. The results presented in figure 2 have been summarized in figure 4 to show some important parameters as functions of Mach number. The slope parameters in this figure have been measured at zero lift.

Ames Aeronautical Laboratory,
National Advisory Committee for Aeronautics,
Moffett Field, Calif.

REFERENCES

1. Smith, Donald W., and Heitmeyer, John C.: Lift, Drag, and Pitching Moment of Low-Aspect-Ratio Wings at Subsonic and Supersonic Speeds - Plane Triangular Wing of Aspect Ratio 2 With NACA 0008-63 Section. NACA RM A50K20, 1951.

2. Smith, Donald W., and Heitmeyer, John C.: Lift, Drag, and Pitching Moment of Low-Aspect-Ratio Wings at Subsonic and Supersonic Speeds - Plane Triangular Wing of Aspect Ratio 2 With NACA 0005-63 Section. NACA RM A50K21, 1951.

3. Heitmeyer, John C., and Stephenson, Jack D.: Lift, Drag, and Pitching Moment of Low-Aspect-Ratio Wings at Subsonic and Supersonic Speeds - Plane Triangular Wing of Aspect Ratio 4 With NACA 0005-63 Section. NACA RM A50K24, 1951.

4. Phelps, E. Ray, and Smith, Willard G.: Lift, Drag, and Pitching Moment of Low-Aspect-Ratio Wings at Subsonic and Supersonic Speeds - Triangular Wing of Aspect Ratio 4 With NACA 0005-63 Thickness Distribution, Cambered and Twisted for Trapezoidal Span Load Distribution. NACA RM A50K24b, 1951.

5. Heitmeyer, John C., and Smith, Willard G.: Lift, Drag, and Pitching Moment of Low-Aspect-Ratio Wings at Subsonic and Supersonic Speeds - Plane Triangular Wing of Aspect Ratio 2 With NACA 0003-63 Section. NACA RM A50K24a, 1951.

6. Smith, Willard G., and Phelps, E. Ray: Lift, Drag, and Pitching Moment of Low-Aspect-Ratio Wings at Subsonic and Supersonic Speeds - Triangular Wing of Aspect Ratio 2 With NACA 0005-63 Thickness Distribution, Cambered and Twisted for a Trapezoidal Span Load Distribution. NACA RM A50K27a, 1951.

7. Reese, David E., and Phelps, E. Ray: Lift, Drag, and Pitching Moment of Low-Aspect-Ratio Wings at Subsonic and Supersonic Speeds - Plane Tapered Wing of Aspect Ratio 3.1 With 3-Percent-Thick, Biconvex Section. NACA RM A50K28, 1951.

8. Hall, Charles F., and Heitmeyer, John C.: Lift, Drag, and Pitching Moment of Low-Aspect-Ratio Wings at Subsonic and Supersonic Speeds - Twisted and Cambered Triangular Wing of Aspect Ratio 2 With NACA 0003-63 Thickness Distribution. NACA RM A51E01, 1951.

9. Heitmeyer, John C.: Lift, Drag, and Pitching Moment of Low-Aspect-Ratio Wings at Subsonic and Supersonic Speeds - Plane Triangular Wing of Aspect Ratio 4 With 3-Percent-Thick, Biconvex Section. NACA RM A51D30, 1951.

10. Heitmeyer, John C., and Hightower, Ronald C.: Lift, Drag, and Pitching Moment of Low-Aspect-Ratio Wings at Subsonic and Supersonic Speeds - Plane Triangular Wing of Aspect Ratio 4 With 3-Percent-Thick Rounded Nose Section. NACA RM A51F21, 1951.

11. Heitmeyer, John C.: Lift, Drag, and Pitching Moment of Low-Aspect-Ratio Wings at Subsonic and Supersonic Speeds - Plane Triangular Wing of Aspect Ratio 3 With NACA 0003-63 Section. NACA RM A51H02, 1951.

12. Frick, Charles W., and Olson, Robert N.: Flow Studies in the Asymmetric Adjustable Nozzle of the Ames 6- by 6-foot Supersonic Wing Tunnel. NACA RM A9E24, 1949.

13. Olson, Robert N., and Mead, Merrill H.: Aerodynamic Study of a Wing-Fuselage Combination Employing a Wing Swept Back 63° - Effectiveness of an Elevon on a Longitudinal Control and the Effects of Camber and Twist on the Maximum Lift-Drag Ratio at Supersonic Speeds. NACA RM A50A31a, 1950.

14. Glauert, H.: Wing-Tunnel Interference on Wings, Bodies and Airscrews. R.&M. No. 1566, British, 1933.

15. Herriot, John G.: Blockage Corrections for Three-Dimensional-Flow Closed-Throat Wind Tunnels, With Consideration of the Effect of Compressibility. NACA Rep. 995, 1950. (Formerly NACA RM A7B28)

16. Lessing, Henry C.: Aerodynamic Study of a Wing-Fuselage Combination Employing a Wing Swept Back 63° - Effect of Sideslip on Aerodynamic Characteristics at a Mach Number of 1.4 With the Wing Twisted and Cambered. NACA RM A50F09, 1950.

17. Perkins, Edward W.: Experimental Investigation of the Effects of Support Interference on the Drag of Bodies of Revolution at a Mach Number of 1.5. NACA TN 2292, 1951. (Formerly NACA RM A8B05)

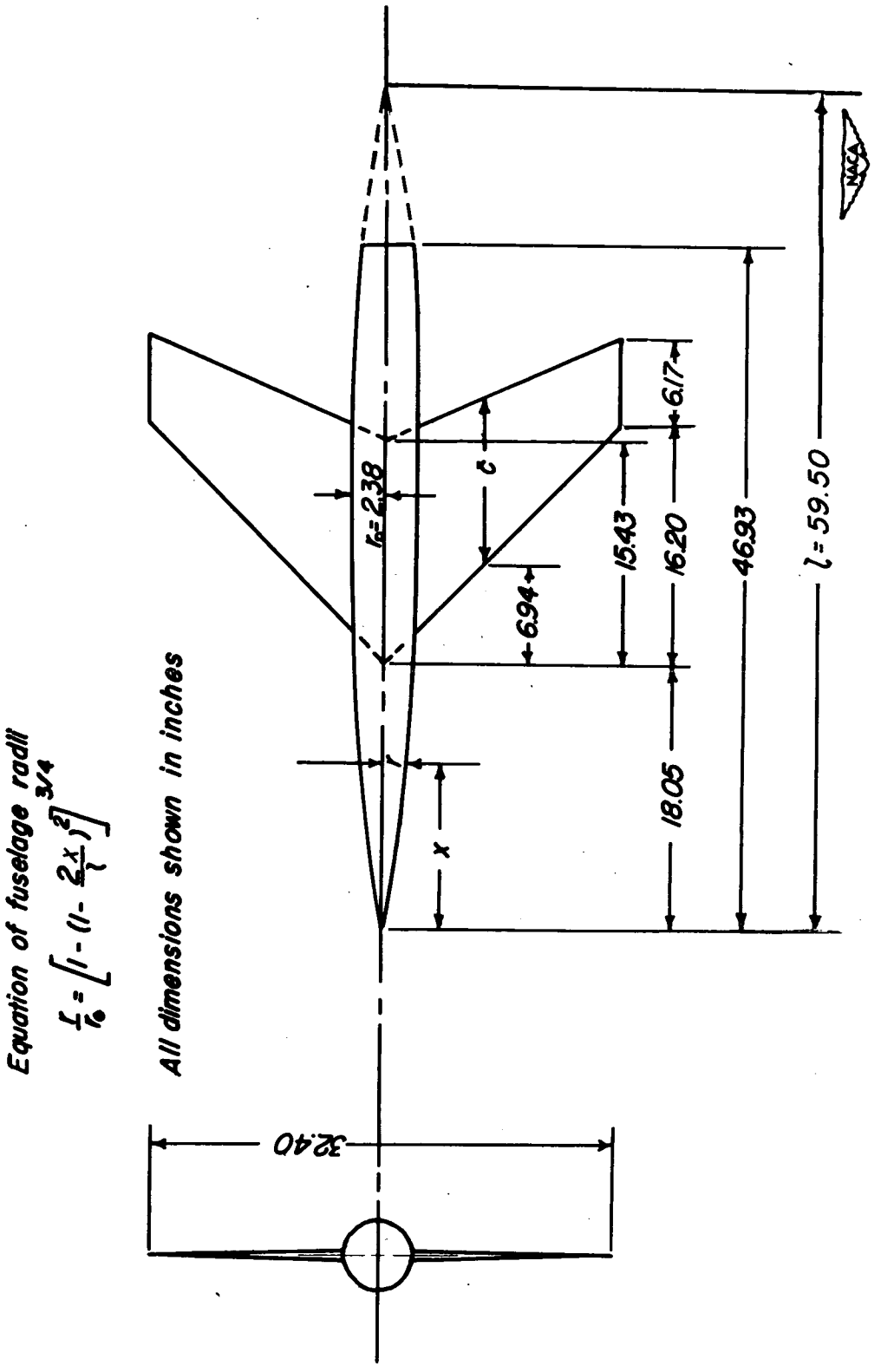

Figure 1.— Front and plan views of the model

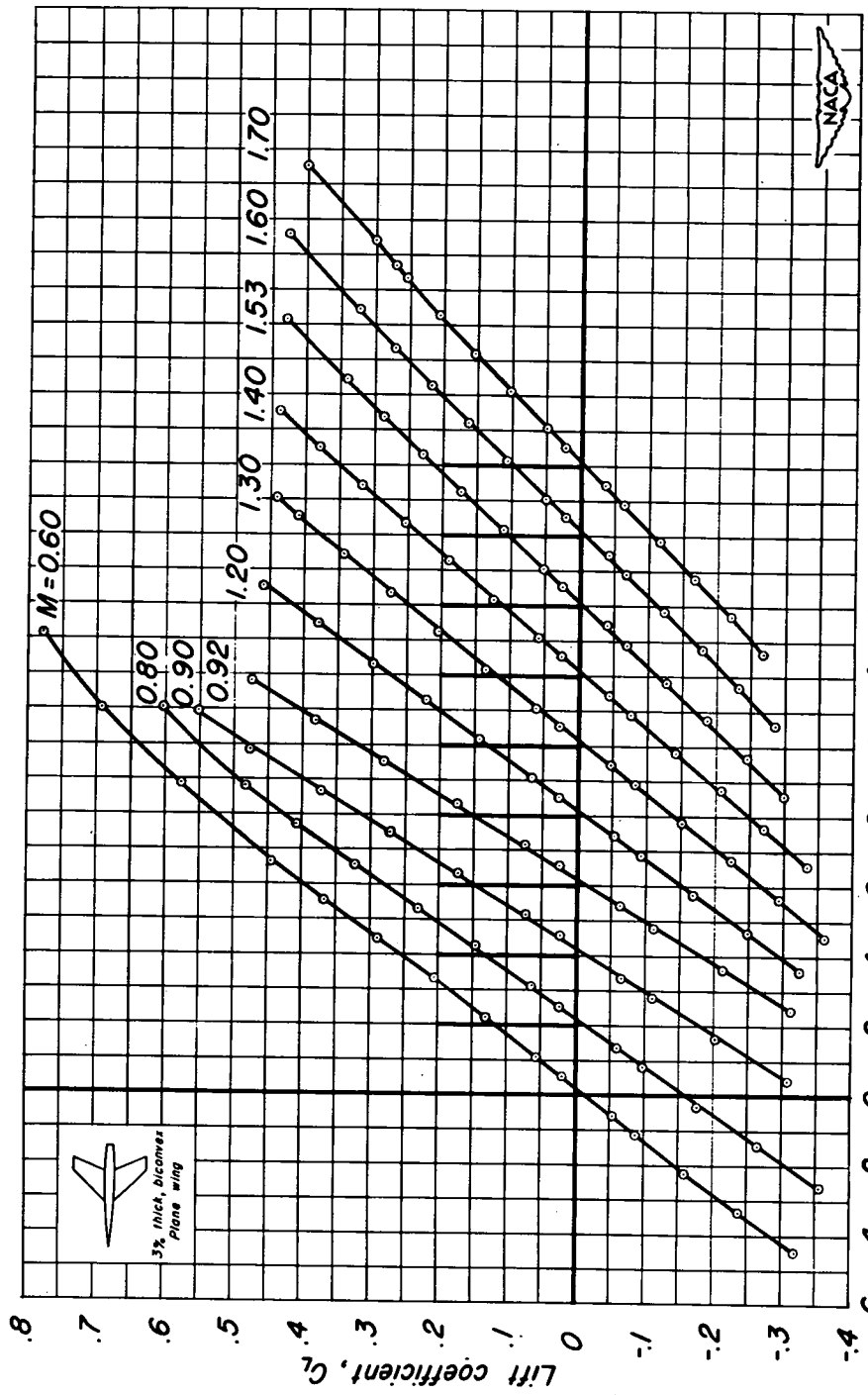

(a) C_L vs α

Figure 2.—The variation of the aerodynamic characteristics with lift coefficient at various Mach numbers. Reynolds number, 3.83 million.

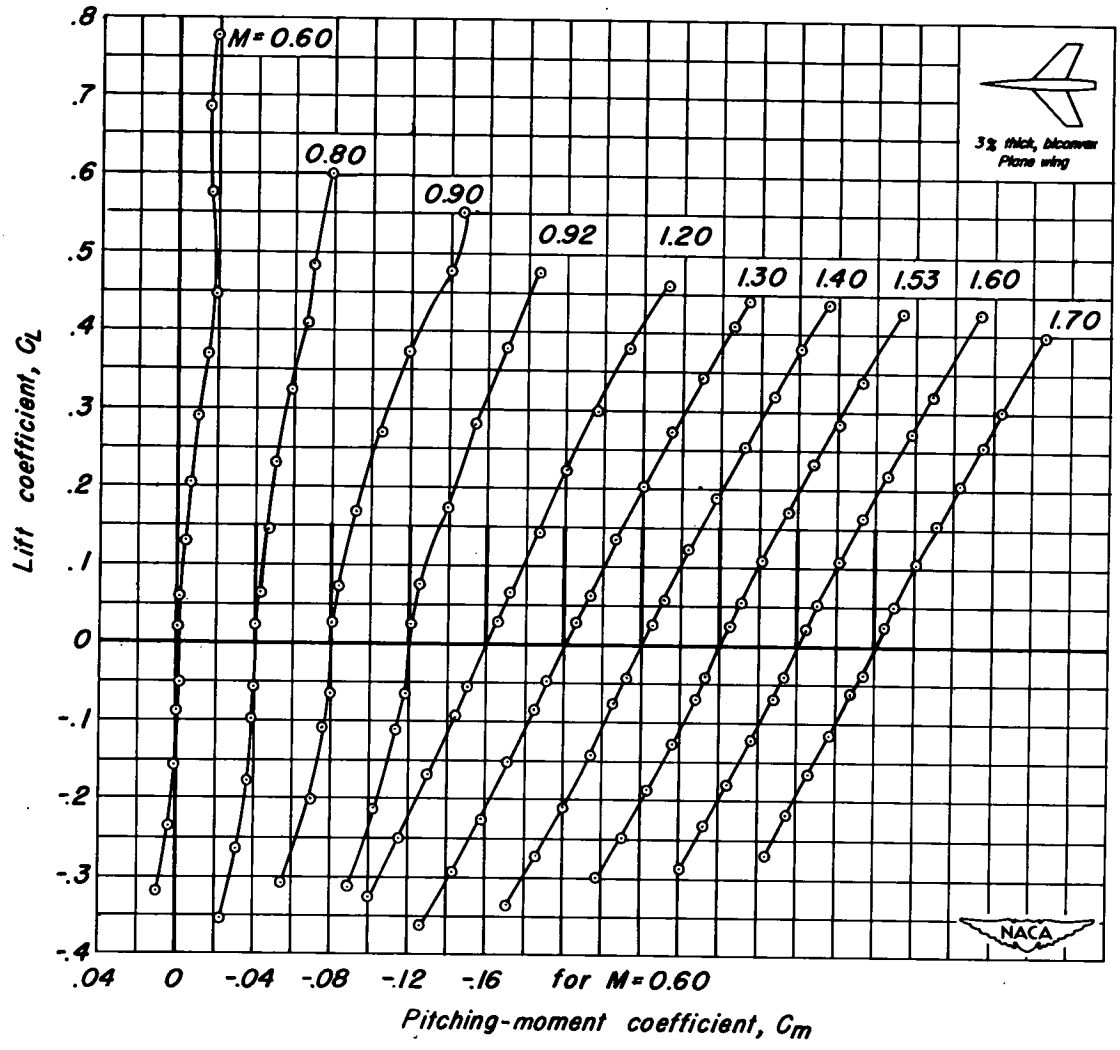

(b) C_L vs C_m

Figure 2.- Continued.

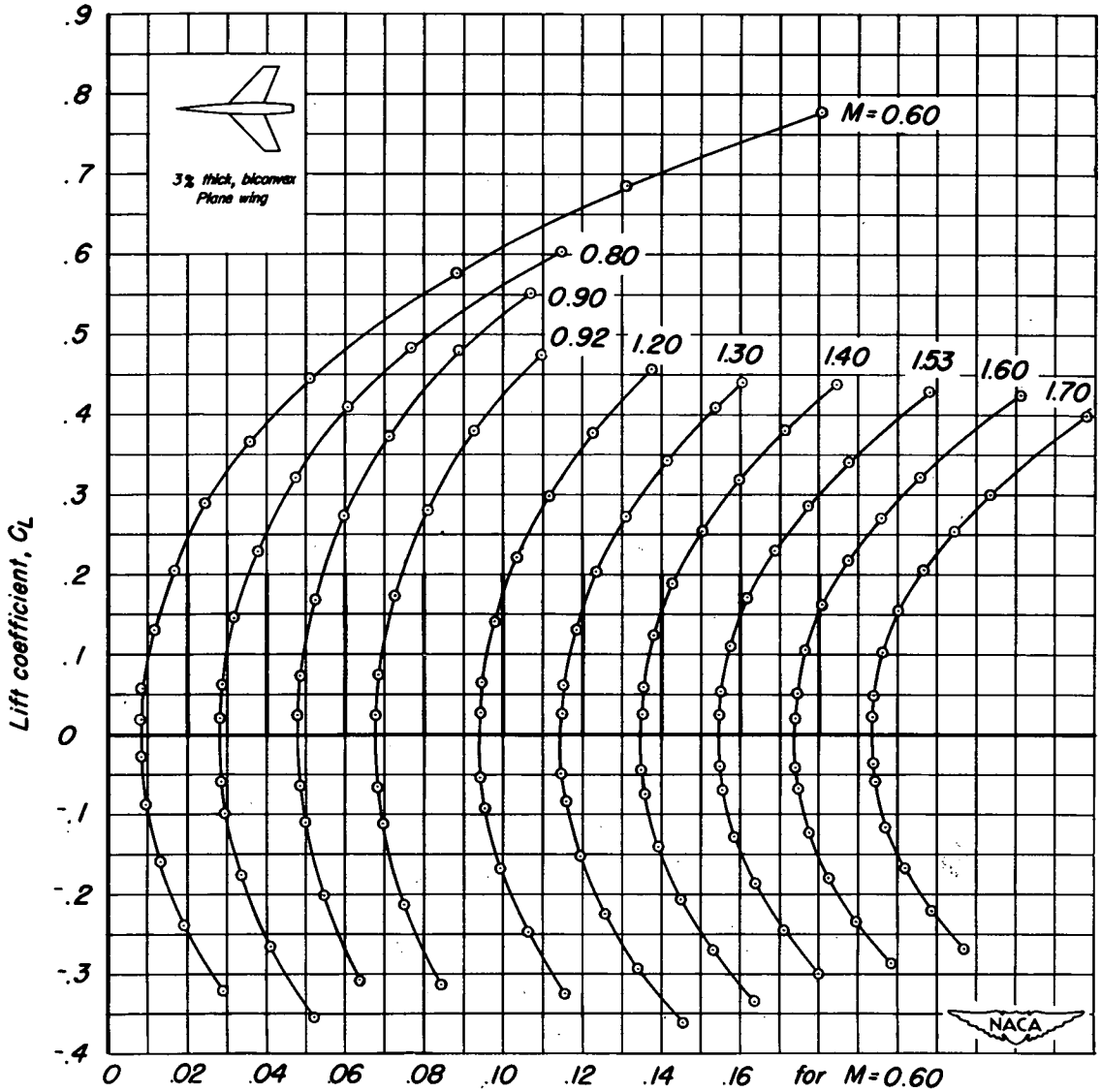

(c) C_L vs C_D

Figure 2.- Continued.

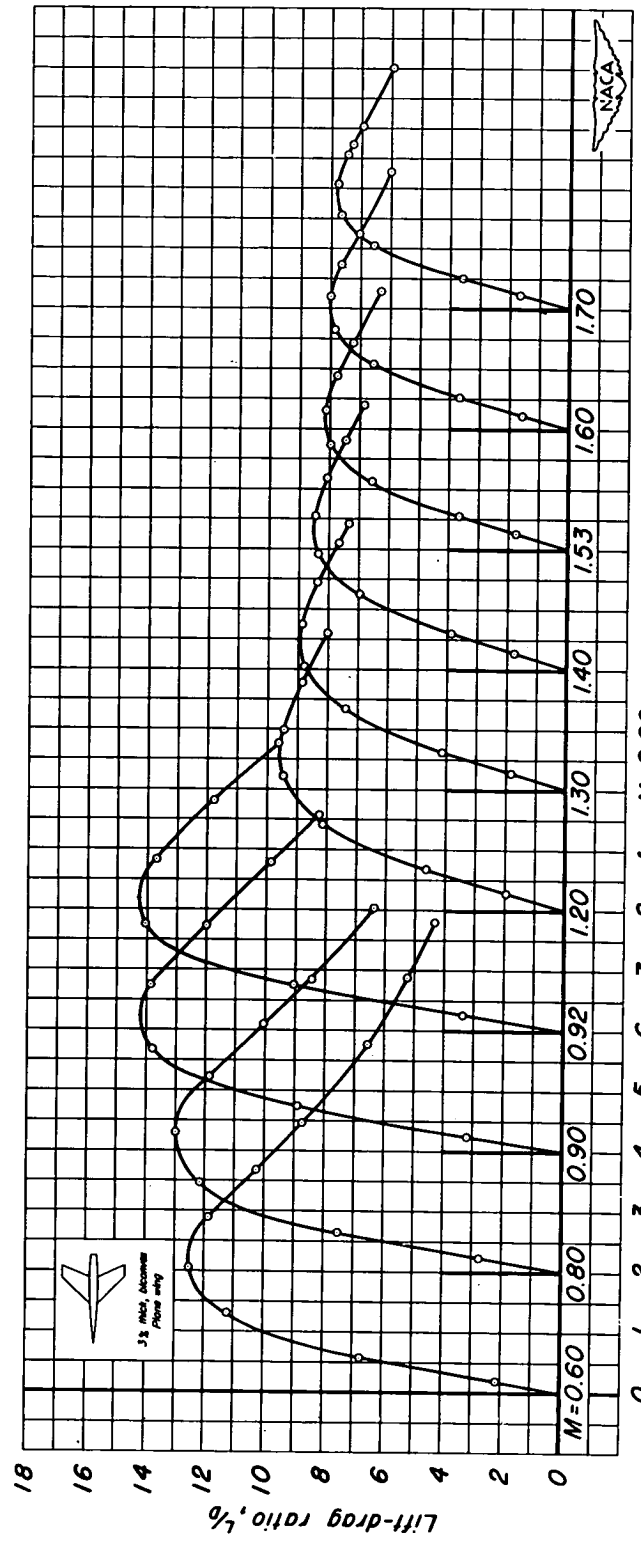

(d) L/D vs C_L

Figure 2.- Concluded.

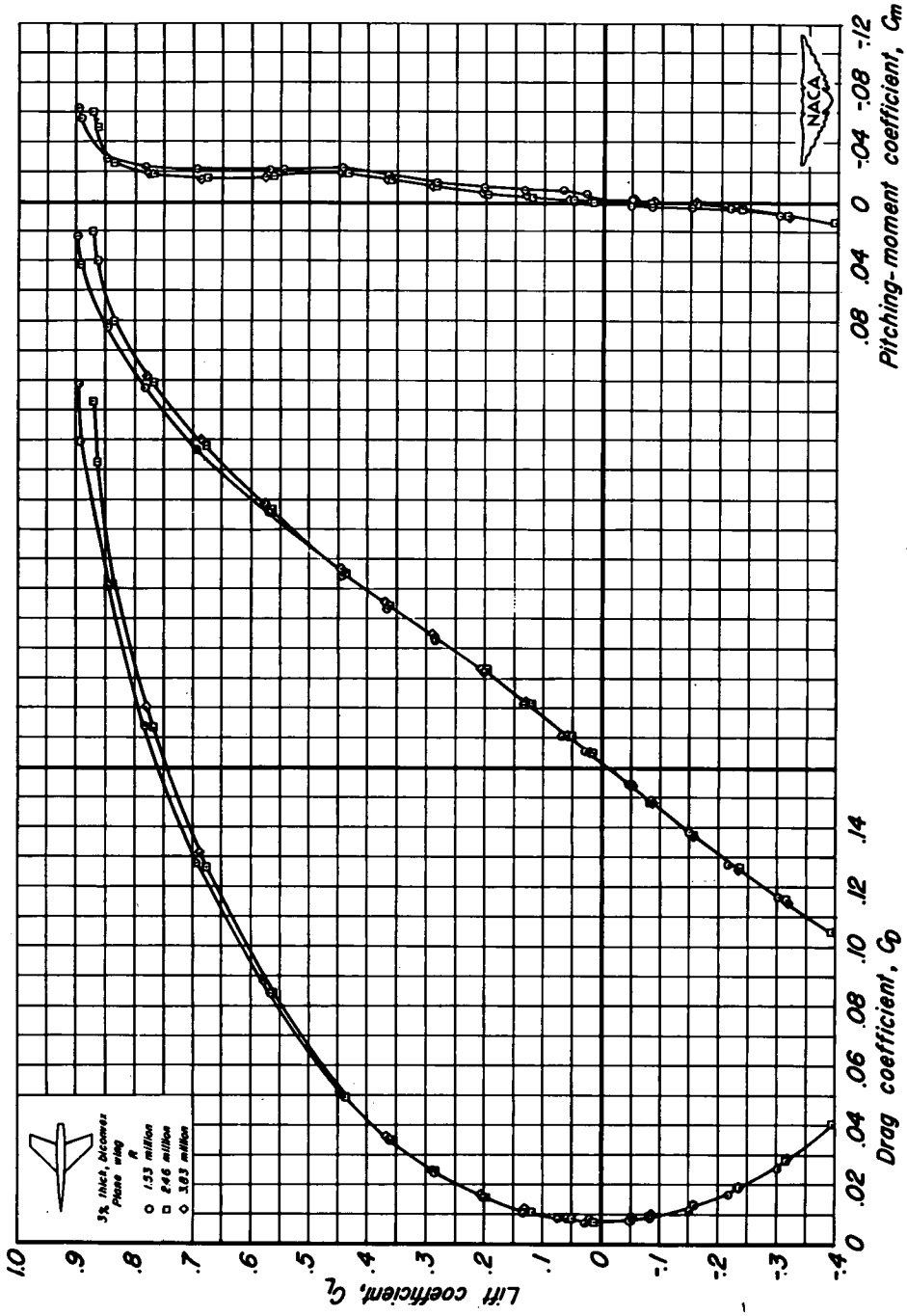

(a) M = 0.60

Figure 3.- The variation of the aerodynamic characteristics with lift coefficient at various Reynolds numbers.

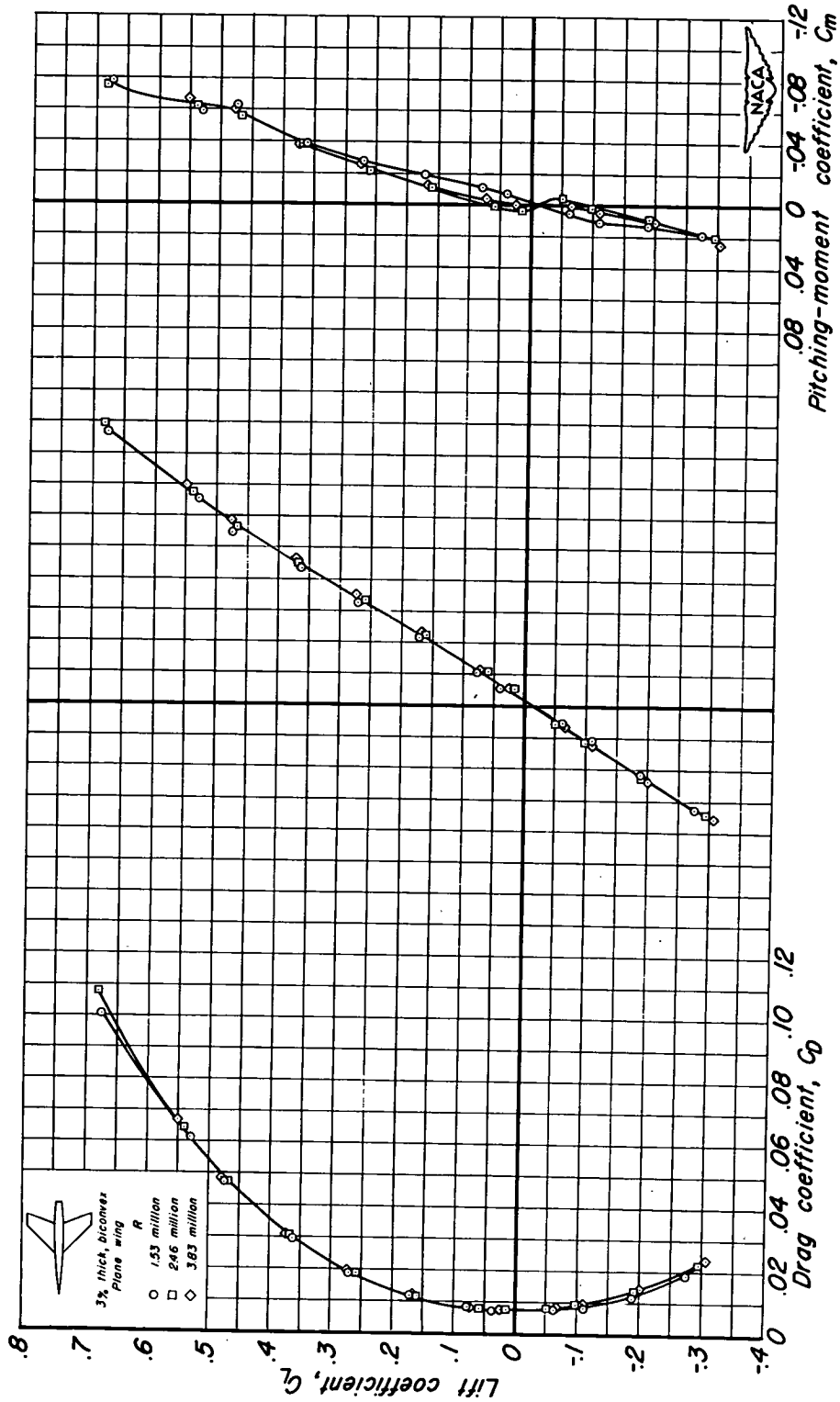

(b) M = 0.90

Figure 3.- Continued.

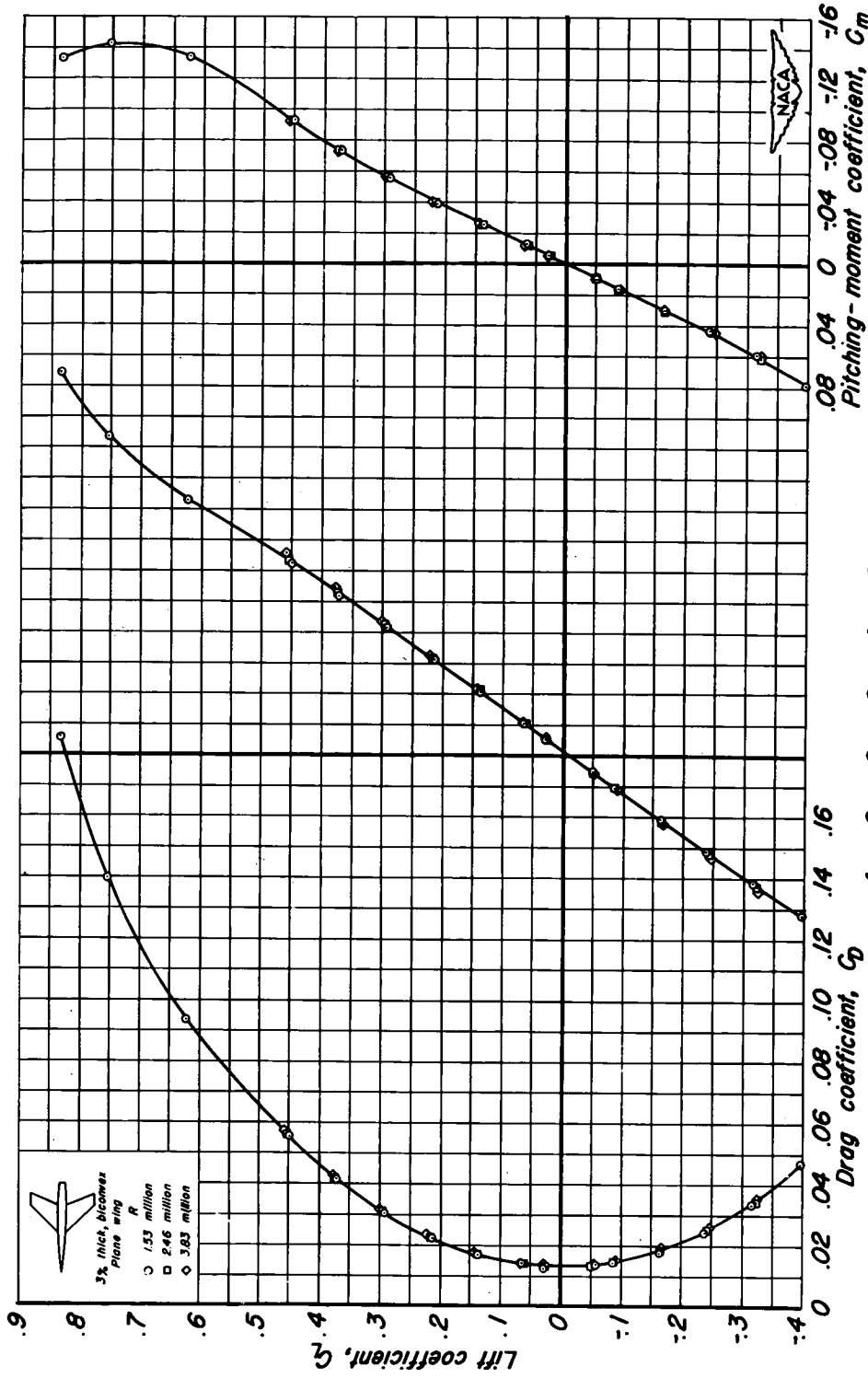

(d) M = 1.20

Figure 3.- Continued.

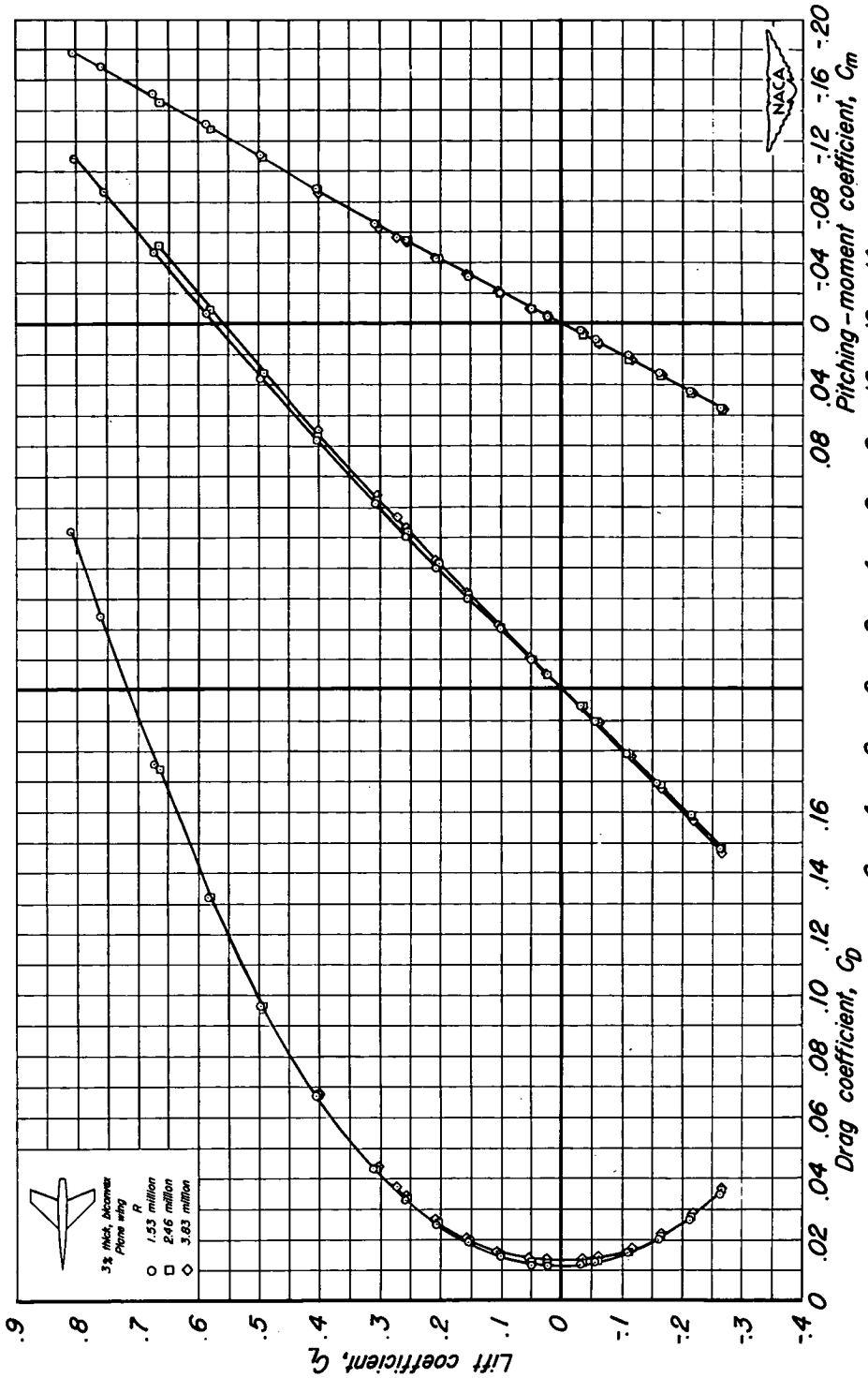

(d) M = 1.70

Figure 3.- Concluded.

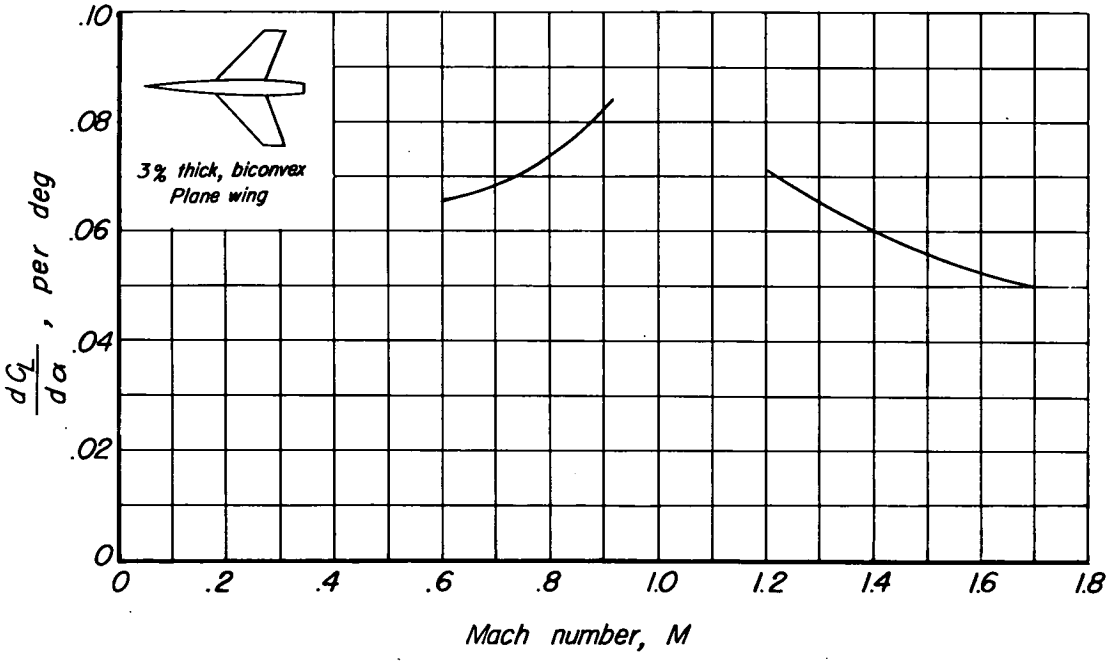

(a) $\frac{dC_L}{d\alpha}$ vs M

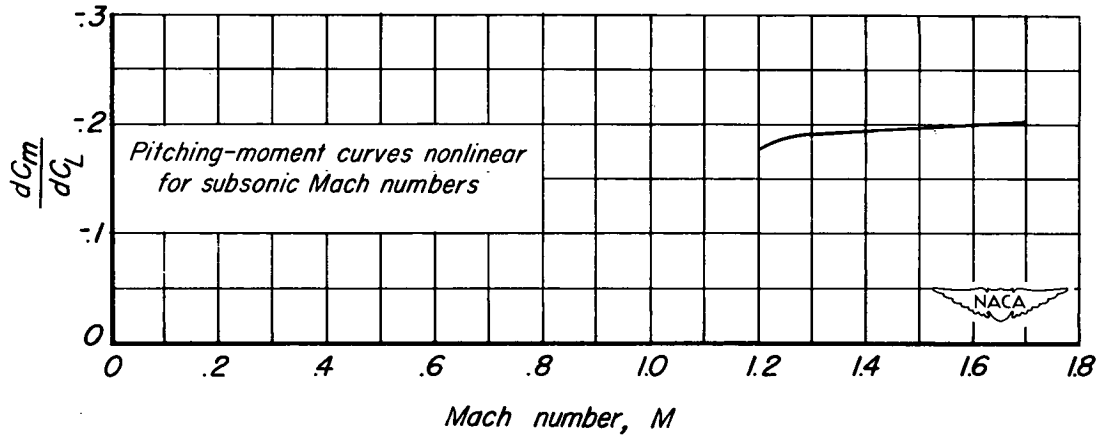

(b) $\frac{dC_m}{dC_L}$ vs M

Figure 4.- Summary of aerodynamic characteristics as a function of Mach number. Reynolds number, 3.83 million.

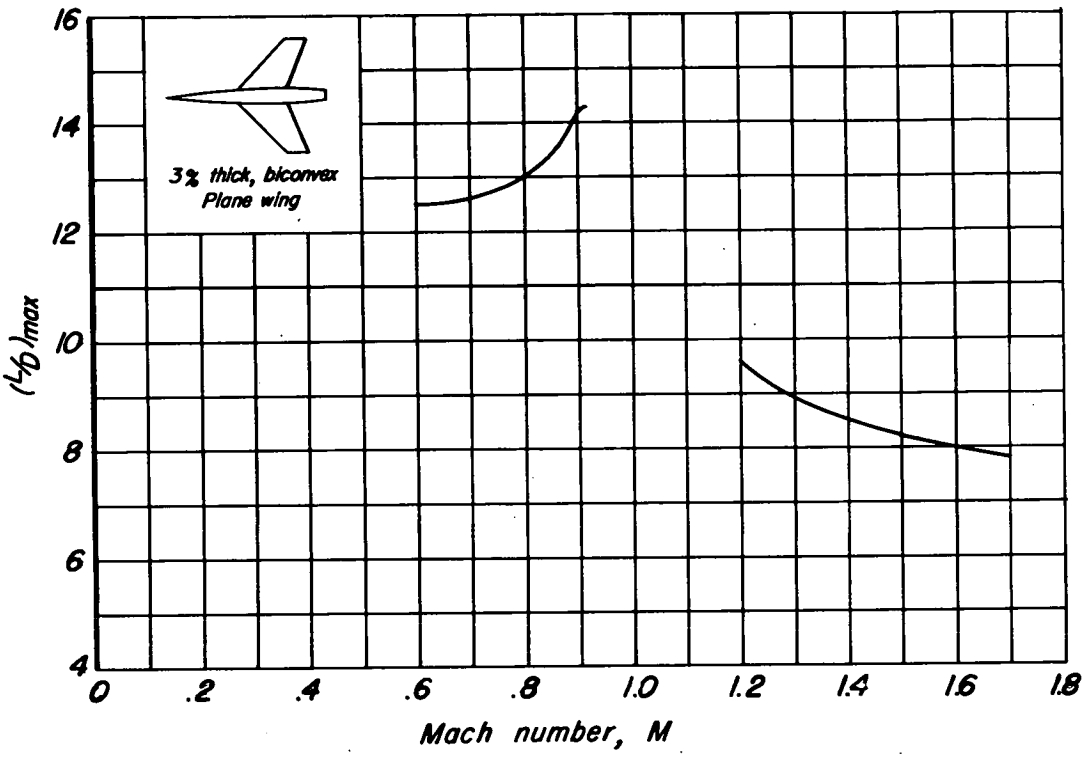

(c) $(L/D)_{max}$ vs M

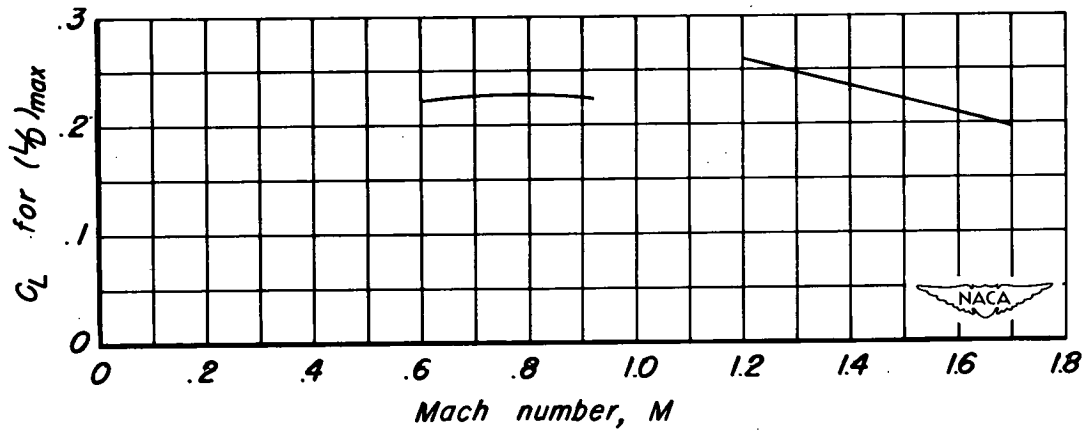

(d) C_L for $(L/D)_{max}$ vs M

Figure 4.- Continued.

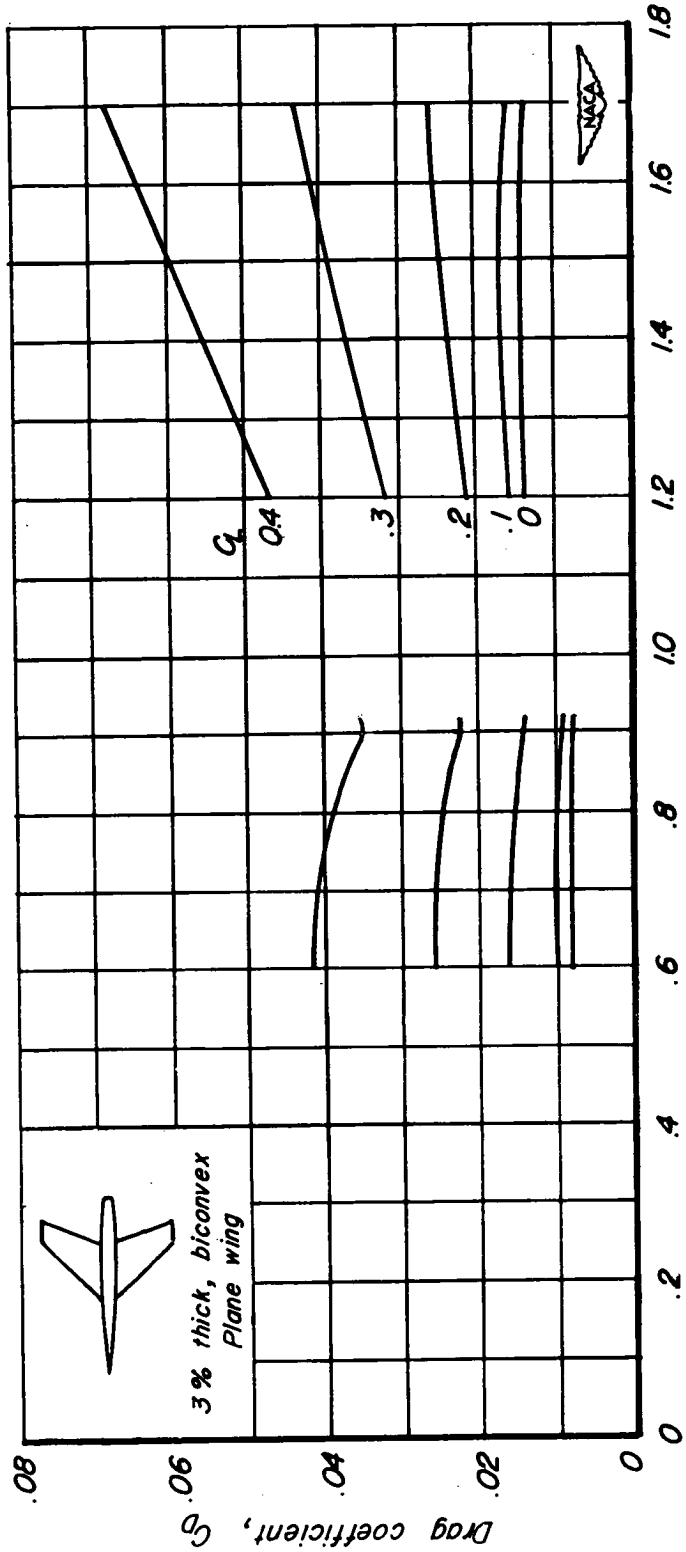

(e) C_D vs M

Figure 4.- Concluded.